In preparation for: Int J Biochem Cell Biol

2017-08-19; Version 19

Full-length review

Mitochondrial respiratory control:

a conceptual perspective on coupling states in mitochondrial preparations.

MitoEAGLE recommendations Part 1

MitoEAGLE Terminology Group

Corresponding author: E. Gnaiger

Contributing co-authors (*alphabetical, to be extended*):

M.G. Alves, D. Ben-Shachar, G.C. Brown, G.R. Buettner, E. Calabria, A.J. Chicco, P.M. Coen, J.L. Collins, L. Crisóstomo, M.S. Davis, C. Doerrier, E. Elmer, A. Filipovska, P.M. Garcia-Roves, D.K. Harrison, K.T. Hellgren, C.L. Hoppel, J. Iglesias-Gonzalez, P. Jansen-Dürr, B.H. Goodpaster, B.A. Irving, S. Iyer, T. Komlodi, V. Laner, H.K. Lee, H. Lemieux, A.T. Meszaros, N. Moisoi, A. Molina, A.L. Moore, A.J. Murray, J. Neuzil, R.K. Porter, K. Nozickova, P.J. Oliveira, K. Renner-Sattler, J. Rohlena, D. Salvadego, L.A. Sazanov, O. Sobotka, R. Stocker, I. Szabo, M. Tanaka, L. Tretter, B. Velika, A.E. Vercesi, Y.H. Wei

Supporting co-authors (*alphabetical*):

P. Bernardi, R.A. Brown, T. Dias, G. Distefano, H. Dubouchaud, Z. Gan, L.F. Garcia-Souza, T. Käämbre, G. Keppner, A. Krajcova, M. Markova, J. Muntané, D. O'Gorman, M.T. Oliveira, C.M. Palmeira, P.X. Petit, K. Siewiera, P. Stankova, Z. Sumbalova

Mitochondrial respiratory control: MitoEAGLE recommendations 1

Correspondence: E. Gnaiger

Department of Visceral, Transplant and Thoracic Surgery, D. Swarovski Research Laboratory, Medical University of Innsbruck, Innrain 66/4, A-6020 Innsbruck, Austria

Email: erich.gnaiger@i-med.ac.at

Tel: +43 512 566796, Fax: +43 512 566796 20

Abstract

Clarity of concepts and consistency of nomenclature are trademarks of the quality of a research field across its specializations, facilitating transdisciplinary communication and education. As research and knowledge on mitochondrial physiology expand, the necessity for harmonization of nomenclature on mitochondrial respiratory states and rates has become apparent. Peter Mitchell's concept of the protonmotive force establishes the link between the electrical and chemical components of energy transformation and coupling in oxidative phosphorylation. This unifying concept provides the framework for developing a consistent terminology on mitochondrial physiology and bioenergetics. We follow IUPAC guidelines on general terms of physical chemistry, extended by concepts of open systems and irreversible thermodynamics. The nomenclature of classical bioenergetics on respiratory states 1 to 5 in an experimental protocol is incorporated into a concept-driven constructive terminology to address the meaning of each respiratory state. Hence we focus primarily on the conceptual 'why' along with clarification of the experimental 'how'. The capacity of *oxidative phosphorylation,* OXPHOS, provides diagnostic reference values and is, therefore, measured at kinetically saturating concentrations of ADP and inorganic phosphate. The contribution of *nonphosphorylating* oxygen consumption is most easily studied by arresting phosphorylation, when oxygen consumption compensates mainly for the proton leak, and the corresponding states are collectively classified as LEAK states. The *oxidative* capacity of the electron transfer system, ETS, reveals the limitation of OXPHOS capacity mediated by the capacity of the *phosphorylation* system. Experimental standards for evaluation of respiratory coupling states must be followed for the development of databases of mitochondrial respiratory function.

Keywords: Mitochondrial respiratory control, coupling control; mitochondrial preparations, protonmotive force, chemiosmotic theory, oxidative phosphorylation,

efficiency; electron transfer system, ETS; proton leak, LEAK; residual oxygen consumption, ROX; State 2, State 3, State 4.

* Does the public expect that biologists understand Darwin's theory of evolution?
* Do students expect that researchers of bioenergetics can explain Mitchell's theory of chemiosmotic energy transformation?

Mitochondria, mt: (Greek mitos: thread; chondros: granule) are small organelles of eukaryotic cells with a double membrane separating the intermembrane space and the matrix with tubular or disk-shaped cristae. Mitochondria maintain their nucleus-independent mtDNA and function as powerhouses and electrochemical generators in cell respiration or oxidative phosphorylation. Abbreviation: mt, as generally used in mtDNA. Mitochondrion is singular and mitochondria is plural. Mitochondria contain the cytochrome system and ATP synthase or alternative oxidases, the enzymes of the tricarboxylic acid cycle with several dehydrogenases, fatty acid oxidation, and ion transporters including proton pumps in particular, besides many other components present in mitochondria. Mitochondria are the oxygen consuming organelles, where the reduction of O_2 is electrochemically coupled to conservation of energy in the form of ATP (oxidative phosphorylation; OXPHOS). Mitochondria are partially independent organelles, yet there is a constant crosstalk between them and the cell. Most of their proteins are encoded by the nuclear DNA, and different cellular signaling pathways, such as Ca^{2+} and protein kinases, modulate mitochondrial activity and structure. In addition, mitochondria interact with each other by fusion and fission all affecting their activity and cell respiration. The bioblasts of Richard Altmann (1894) are not only the mitochondria as presently defined, but include symbiotic and free-living bacteria. “For the physiologist, mitochondria afforded the first opportunity for an experimental approach to structure-function relationships, in particular those involved in active transport, vectorial metabolism, and metabolic control mechanisms on a subcellular level” (Ernster and Schatz 1981).

1. Introduction

Every study of mitochondrial function and disease in tissues and cells is faced with **e**volution, **a**ge, **g**ender, **l**ifestyle and **e**nvironment (EAGLE) as essential background conditions characterizing the individual patient or subject, cohort, species, tissue and to some extent even cell line. As a large and highly coordinated group of laboratories and researchers, the global MitoEAGLE network is uniquely poised to generate the necessary scale, type, and quality of consistent data sets to address this intrinsic complexity. The mission of the MitoEAGLE network aims at developing harmonized experimental protocols and implementing a quality control and data management system to interrelate results obtained in different studies and to generate a rigorously monitored database focused on mitochondrial respiratory function.

Reliability and comparability of quantitative results depends on the accuracy of measurement under well-defined conditions. A conceptually meaningful framework is required to relate the results of experiments carried out by different research groups. Vague or ambiguous terminology can lead to confusion and may relegate valuable signals to wasteful noise. For this reason, measured values must be expressed in standardized units for each parameter used to define mitochondrial respiratory control. Standardization of nomenclature and technical jargon is essential to improve the awareness of the intricate meaning of divergent scientific vocabulary. The MitoEAGLE Terminology Group aims at accomplishing the ambitious goal to harmonize, unify and thus simplify the terminology in the field of mitochondrial physiology. A focus on coupling states in mitochondrial preparations can be considered as a first step in the attempt to generate a harmonized and conceptually oriented nomenclature in bioenergetics and mitochondrial physiology. Comparison with coupling states of intact cells (Wagner *et al.* 2011) and respiratory control by fuel substrates and specific inhibitors of respiratory enzymes (Gnaiger 2009; 2014) will be reviewed in subsequent recommendations.

Mitochondrial preparations are defined as tissue or cellular preparations in which the plasma membrane is either removed (isolated mitochondria), or mechanically and/or chemically permeabilized (tissue homogenate, permeabilized fibres, permeabilized cells), while the functional integrity and to a large extent the structure of mitochondria are maintained.

2. Fundamental respiratory coupling states in mitochondrial preparations

> '*Every professional group develops its own technical jargon for talking about matters of critical concern ... People who know a word can share that idea with other members of their group, and a shared vocabulary is part of the glue that holds people together and allows them to create a shared culture*' (Miller 1991).

2.1. Definitions

Respiratory control is exerted in a mitochondrial preparation by experimental conditions defined as respiratory states. Coupling states in mitochondrial preparations depend on the exogenous supply of fuel substrates and oxygen to support the electron transfer system, ETS (**Fig. 1**). Phosphorylation of ADP to ATP is stimulated or depressed which causes an increase or decrease of electron flow linked to oxygen consumption in 'controlled' coupling states. Alternatively, coupling of electron transfer with phosphorylation is disengaged by uncouplers, functioning like a clutch in a mechanical system. The corresponding 'uncontrolled' state is characterized by high levels of dissipative oxygen consumption without conservation of energy (**Fig. 2**). Such uncoupling is different from switching to mitochondrial pathways that involve less than three coupling sites, bypassing Complex I through multiple electron entries into the Q-junction (**Fig. 1**). A bypass of the third coupling site (Complex IV) is provided by alternative oxidases, which reduce oxygen without proton translocation. Reprogramming mitochondrial pathways may be considered as a switch of gears (stoichiometry) rather than uncoupling (loosening the stoichiometry).

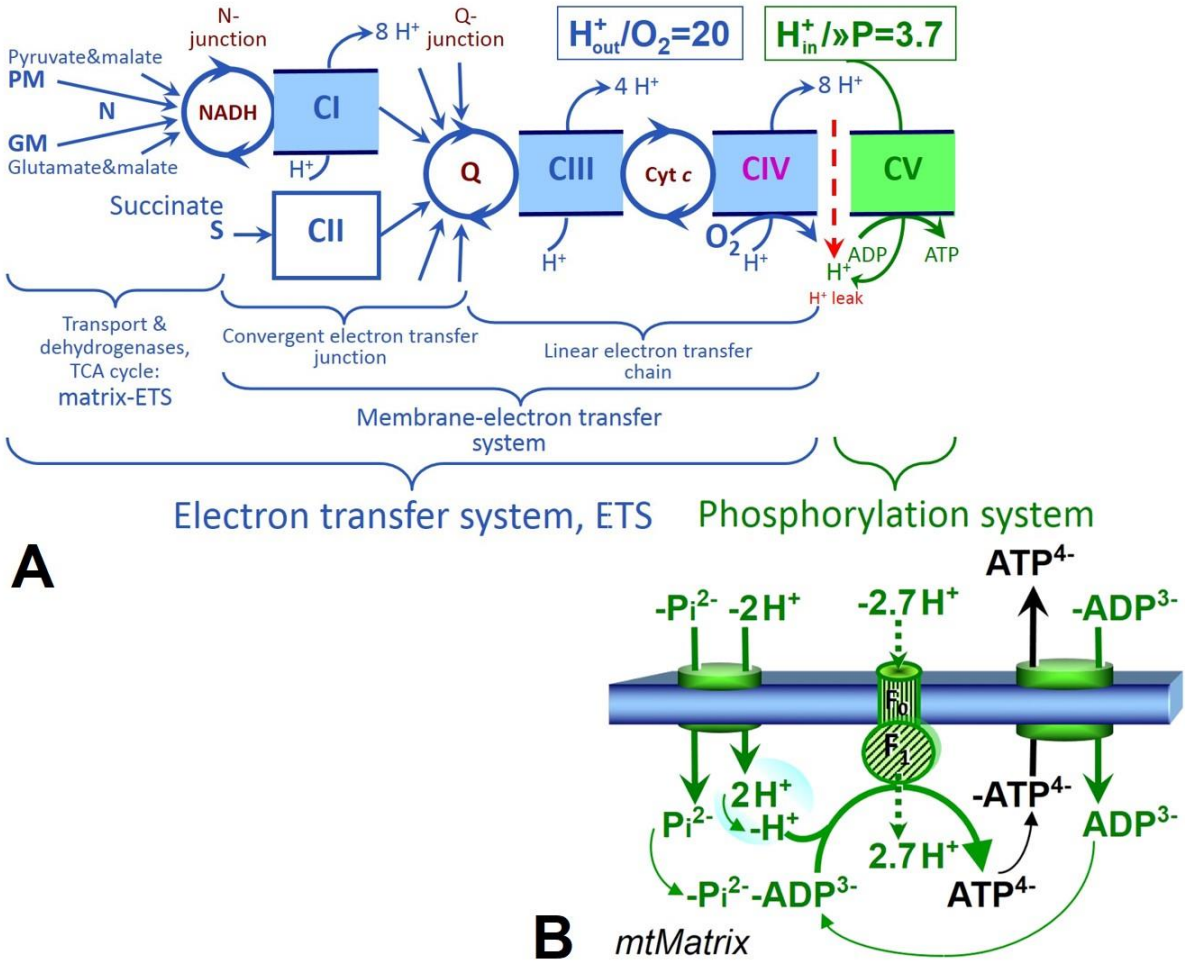

Fig. 1. The mitochondrial respiratory system. In oxidative phosphorylation the electron transfer system, ETS (**A**; *to be updated by L Sazalov*) is coupled to the phosphorylation system (**B**). See Eqs. 4 and 5 for further explanation. Modified from (A) Lemieux *et al.* (2017) and (B) Gnaiger (2014).

Phosphorylation, »P: *Phosphorylation* in the context of OXPHOS is clearly defined as phosphorylation of ADP to ATP. On the other hand, the term phosphorylation is used in the general literature in many different contexts (phosphorylation of enzymes, *etc*.). This justifies consideration of a symbol more discriminative than P as used in the P/O ratio (phosphate to atomic oxygen ratio), where P indicates phosphorylation of ADP to ATP or GDP to GTP. We propose the symbol »P for the energetic uphill direction of phosphorylation coupled to catabolic reactions, and likewise the symbol «P for the corresponding downhill reaction (**Fig.**

2). ATP synthase is the most important enzyme complex of the phosphorylation system (**Fig. 1B**), and »P may also involve substrate-level phosphorylation as part of the tricarboxylic acid cycle (succinyl-CoA ligase), in the matrix (phosphoenylpyruvate carboxykinase) and cytosol (pyruvate kinase, phosphoglycerate kinase). ADP is formed in the adenylate kinase reaction, 2 ADP ↔ ATP + AMP. In isolated mammalian mitochondria ATP production catalysed by adenylate kinase proceeds without fuel substrates in the presence of ADP (Komlódi and Tretter 2017).

Control and regulation: The terms metabolic *control* and *regulation* are frequently used synonymously, but are distinguished in metabolic control analysis: '*We could understand the regulation as the mechanism that occurs when a system maintains some variable constant over time, in spite of fluctuations in external conditions (homeostasis of the internal state). On the other hand, metabolic control is the power to change the state of the metabolism in response to an external signal*' (Fell 1997). Respiratory control may be exerted by: (*1*) ATP demand (**Fig. 2**); (*2*) fuel substrate, pathway competition and oxygen availability (starvation and hypoxia); (*3*) the protonmotive force, redox states, flux-force relationships, coupling and efficiency; (*4*) mitochondrial enzyme activities and allosteric regulation by adenylates, phosphorylation of regulatory enzymes, Ca^{2+} and other ions including H^{+}; (*5*) inhibitors (*e.g.* NO or intermediary metabolites, such as oxaloacetate); (*6*) enzyme content, concentrations of cofactors and conserved moieties (such as adenylates, NADH/NAD^{+}, coenzyme Q, cytochrome *c*); (*7*) metabolic channeling by supercomplexes; and *(8)* mitochondrial density (enzyme concentrations and membrane area) and morphology (fission and fusion). Regulation by hormone concentrations, gender and life style, and by genetic or acquired diseases causing mitochondrial dysfunction exerts an influence on all control mechanisms listed above (for reviews, see Brown 1992; Gnaiger 1993a, 2009; 2014; Morrow *et al*. 2017).

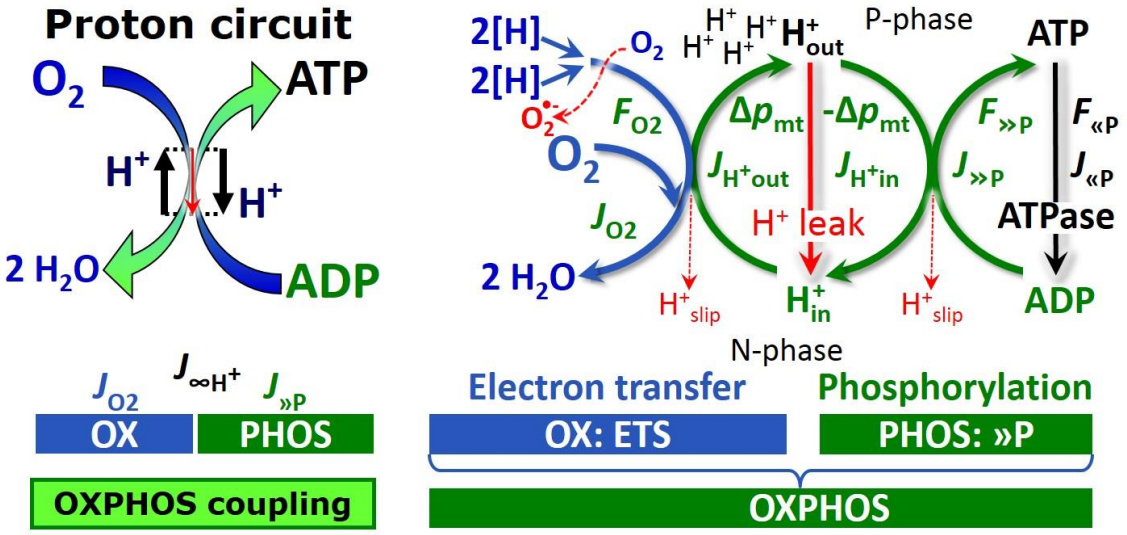

Fig. 2. The proton circuit and coupling in oxidative phosphorylation (OXPHOS). Oxygen flux, J_{O2}, is coupled to the phosphorylation of ADP to ATP, $J_{»P}$, by the proton pumps of the electron transfer system, ETS, pushing the outwards proton flux, J_{H+out}, and generating the protonmotive force, Δp_{mt}. ATP synthase is driven by the protonmotive force, $-\Delta p_{mt}$, and inwards proton flux, J_{H+in}, to phosphorylate ADP to ATP. 2[H] indicates the reduced hydrogen equivalents of fuel substrates that provide the chemical input force, F_{O2} [kJ/mol O_2], of the reaction with oxygen (molar Gibbs energy of reaction), typically in the range of -460 to -480 kJ/mol. The output force is given by the phosphorylation potential difference, $F_{»P}$ [kJ/mol ADP phosphorylated to ATP], which varies *in vivo* in the range of about 48 to 62 kJ/mol under physiological conditions. Proton turnover, $J_{\infty H+}$, and ATP turnover, $J_{\infty P}$, proceed in the steady state at constant Δp_{mt}, when $J_{\infty H+} = J_{H+out} = J_{H+in}$, and at constant $F_{»P}$, when $J_{\infty P} = J_{»P} = J_{«P}$. $J_{»P}/J_{O2}$ (»P/O_2) is two times the 'P/O' ratio of classical bioenergetics. The effective »P/O_2 ratio is diminished by: (*1*) the proton leak across the inner mitochondrial membrane from low pH in the P-phase to high pH in the N-phase (P, positive; N, negative); (*2*) cycling of other cations; (*3*) proton slip of the proton pumps when effectively a proton is not pumped; and (*4*) electron leak in the univalent reduction of oxygen to superoxide anion radical ($O2^{\bullet-}$). Modified from Gnaiger (2014).

2.2. Classical terminology for isolated mitochondria

> *'When a code is familiar enough, it ceases appearing like a code; one forgets that there is a decoding mechanism. The message is identical with its meaning'* (Hofstadter 1979).

Chance and Williams (1955; 1956) introduced five classical states of mitochondrial respiration and cytochrome redox states. **Table 1** shows a protocol with isolated mitochondria in a closed respirometric chamber, defining a consecutive sequence of respiratory states.

State 1 is obtained after addition of isolated mitochondria to air-saturated isoosmotic/isotonic respiration medium containing inorganic phosphate, but no adenylates (*i.e.* AMP, ADP, ATP) and no fuel substrates.

State 2 is induced by addition of a high concentration of ADP (typically 100 to 300 µM), which stimulates respiration transiently on the basis of endogenous fuel substrates and phosphorylates only a small portion of the added ADP. State 2 is then obtained at a low respiratory activity limited by zero endogenous fuel substrate availability (**Table 1**). If addition of specific inhibitors of respiratory complexes, such as rotenone, do not cause a further decline of oxygen consumption, State 2 is equivalent to residual oxygen consumption (see below). If inhibition is observed, undefined endogenous fuel substrates are a confounding factor of pathway control by externally added substrates.

State 3 is the state stimulated by addition of fuel substrates while the ADP concentration is still high (**Table 1**) and supports coupled energy transformation through oxidative phosphorylation. 'High ADP' is a concentration of ADP specifically selected to allow the measurement of State 3 to State 4 transitions of isolated mitochondria in a closed respirometric system. A repeated ADP titration re-establishes State 3 at 'high ADP'. Starting at oxygen concentrations near air saturation (ca. 200 µM O_2), the total ADP

concentration added must be low enough (typically 100 to 300 µM) to allow phosphorylation to ATP at a coupled oxygen consumption that does not lead to oxygen depletion during the transition to State 4. In contrast, kinetically saturating ADP concentrations are usually an order of magnitude higher than 'high ADP'.

State 4 is only reached if the mitochondrial preparation is of high quality and is well coupled. Depletion of ADP by phosphorylation to ATP will then lead to a decline in oxygen uptake in the transition from State 3 to State 4. Under these conditions a maximum Δp_{mt} and high ATP/ADP ratio are maintained. State 4 respiration reflects intrinsic proton leak and the ATPase activity.

State 5 is a state obtained after exhaustion of oxygen in a closed respirometric chamber. Oxygen diffusion from the surroundings into the aqueous solution may be a confounding factor preventing complete anoxia (Gnaiger 2001).

Table 1. Metabolic states of mitochondria (after Chance and Williams, 1956).

State	$[O_2]$	[ADP]	[Substrate]	Respiration rate	Rate-limiting substance
1	>0	Low	Low	Slow	ADP
2	>0	High	~0	Slow	Substrate
3	>0	High	High	Fast	Respiratory chain
4	>0	Low	High	Slow	ADP
5	0	High	High	0	Oxygen

2.3. Three coupling states of mitochondrial preparations and residual oxygen consumption

It has been suggested to extend the classical nomenclature (differential: States 1 to 5) by a concept-driven terminology that incorporates explicit information on the nature of the respiratory states (Gnaiger 2009). Coupling states of mitochondrial preparations can be compared in any mitochondrial pathway control state, *i.e.* keeping fuel substrates and ETS inhibitors constant while varying adenylate concentrations and inhibitors of the phosphorylation system (**Fig. 1**). The terminology must be general and not restricted to any

particular experimental protocol or mitochondrial preparation. In the following section, the new concept driven terminology is explained and coupling states are defined.

OXPHOS state (**Fig. 3**): The respiratory state with saturating concentrations of O_2, respiratory and phosphorylation substrates, and zero uncoupler, to provide an estimate of the maximal capacity of OXPHOS in any given pathway control state. Respiratory capacities at saturating substrate concentrations provide reference values or upper limits of performance, aiming at the generation of data sets for comparative purposes. Any effects of substrate kinetics are thus separated from reporting actual mitochondrial capacities, against which physiological activities can be evaluated.

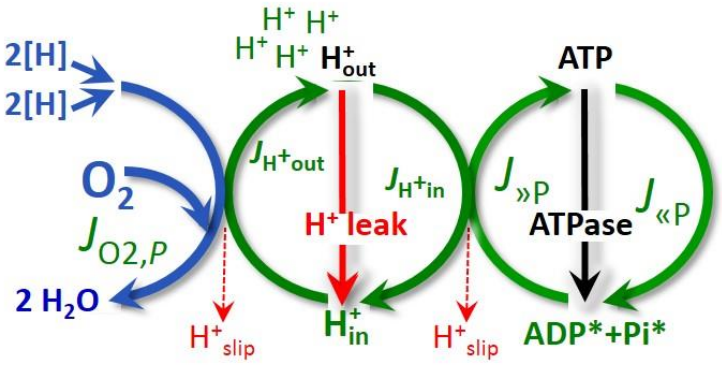

Fig. 3. OXPHOS state when phosphorylation, $J_{»P}$, is supported by a high Δp_{mt}, is stimulated by kinetically saturating [ADP]* and inorganic phosphate, [Pi]*. O_2 flux, $J_{O2,P}$, is highly coupled at a maximum »P/O_2 ratio, $J_{»P}/J_{O2,P}$ (see also Fig. 2).

As discussed previously, 0.2 mM ADP does not fully saturate flux in isolated mitochondria (Gnaiger 2001; Puchowicz *et al.* 2004), and even higher ADP concentrations are required, particularly in permeabilized muscle fibres, to overcome limitations by diffusion and by the tubulin-regulated conductance of the outer mitochondrial membrane (Rostovtseva *et al.* 2008). In permeabilized muscle fibre bundles of high respiratory capacity, the apparent K_m for ADP increases up to 0.5 mM (Saks *et al.* 1998). This implies that >90 % saturation is reached only at >5 mM ADP.

ETS state (**Fig. 4**): The ETS state is defined as the noncoupled state with saturating concentrations of O_2, respiratory substrate and uncoupler, as an estimate of the oxidative capacity of the ETS. Optimal *exogenous* uncoupler concentration for maximum O_2 flux provides the condition for measurement of ETS capacity. As a consequence of the nearly collapsed Δp_{mt}, the driving force for phosphorylation is missing and $J_{»P}=0$. The abbreviation State 3u is used frequently in bioenergetics, to indicate the state of maximum respiration without sufficient emphasis on the fundamental difference between OXPHOS capacity (*well coupled* with an *endogenous* uncoupled component) and ETS capacity (*noncoupled*).

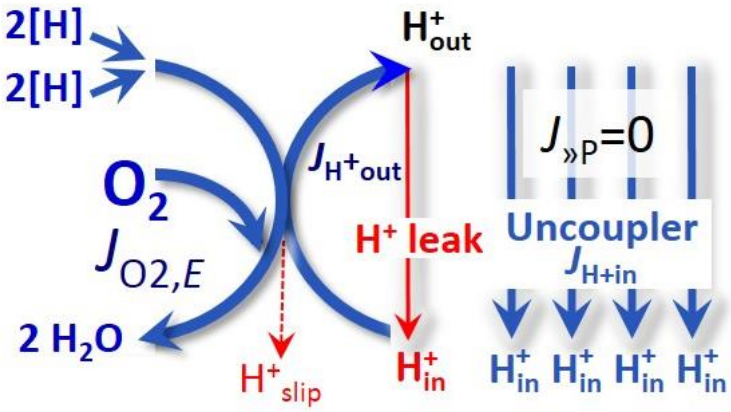

Fig. 4. ETS state when noncoupled respiration, $J_{O2,E}$, is maximum at optimum exogenous uncoupler concentration and phosphorylation is zero, $J_{»P}=0$ (see also Fig. 2).

LEAK state (**Fig. 5**): A state of mitochondrial respiration when O_2 flux is maintained at saturating concentrations of O_2 and respiratory substrates, and zero ATP-turnover without addition of any

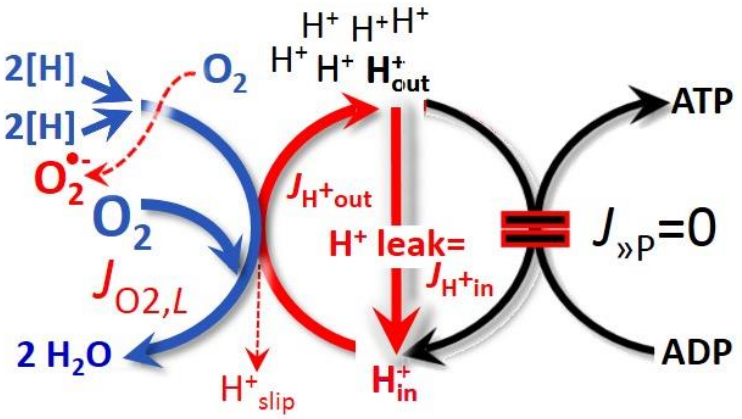

Fig. 5. LEAK state when phosphorylation is arrested, $J_{»P}=0$, and oxygen flux, $J_{O2,L}$, is controlled mainly by the proton leak, which equals J_{H^+in}, at maximum Δp_{mt} (see also Fig. 2).

experimental uncoupler, as an estimate of the maximal proton leak rate. LEAK respiration can be measured: (*1*) in the absence of adenylates; (*2*) after depletion of ADP at maximum ATP/ADP ratio; or (*3*) after inhibition of the phosphorylation system by inhibitors of ATP synthase, such as oligomycin, or adenylate nucleotide translocase, such as carboxyatractyloside. Oxygen consumption in State 4 represents an overestimation of LEAK respiration if the ATPase activity maintains some stimulation of respiration by recycled ADP at $J_{»P}>0$. This can be tested by inhibition of the phosphorylation system using oligomycin, ensuring that $J_{»P}=0$.

Proton leak: Proton leak is the process in which protons are translocated across the inner mitochondrial membrane in the direction of the downhill protonmotive force without coupling to phosphorylation. The proton leak flux depends on Δp_{mt} and is a property of the inner mitochondrial membrane.

Proton slip: Proton slip is the process in which protons are only partially translocated by a proton pump and slip back to the original compartment. The proton slip is a property of the proton pump and depends on the turnover rate of the proton pump.

Besides these three main coupling states, the following respiratory state is also relevant to assess respiratory function:

ROX: Residual oxygen consumption (ROX) is defined as O_2 consumption due to oxidative side reactions remaining after inhibition of the ETS. ROX is not a coupling state but represents a baseline that is used to correct mitochondrial respiration in defined coupling states. ROX is not necessarily equivalent to non-mitochondrial respiration, considering oxygen-consuming reactions in mitochondria not related to ETS, such as oxygen consumption in the reaction catalyzed by monoamine oxidases. In the presence of O_2, ROX is measured either in the absence of fuel substrates or after blocking the electron supply to cytochrome *c* oxidase and alternative oxidases.

Table 2. Coupling states in mitochondrial preparations.

State	Respiration	Δp_{mt}	Induced by:	Limited by:
LEAK	*L*; low, proton leak-dependent respiration	Max	Kinetically saturating [substrate] and [O_2] without ADP or with full inhibition of the ADP phosphorylation system	Proton leak
OXPHOS	*P*; high, ADP-stimulated respiration	High	Kinetically saturating [substrate], [ADP], [P_i] and [O_2]	Phosphorylation system or electron transfer system
ETS	*E*; maximal, noncoupled respiration	Min	Kinetically saturating [substrate] and [O_2] at optimal uncoupler concentration for maximum oxygen flux	Electron transfer system
ROX	*Rox*, Minimum, residual (non-ETS) oxygen consumption	0	Full inhibition of ETS or absence of substrates	Non-ETS oxidation reactions

3. States and rates

3.1. Respiratory states and respiratory rates

Fig. 6 summarizes the three coupling states, ETS, LEAK and OXPHOS, and puts them into a schematic context with the corresponding respiratory rates, abbreviated as *E*, *L* and *P*, respectively. This clarifies that *E* may exceed or be equal to *P*, but *E* cannot theoretically be lower than *P*. *E*<*P* must be discounted as an artefact, which may be caused experimentally by:

(*1*) using too low uncoupler concentrations; (*2*) using high and inhibitory uncoupler concentrations (Gnaiger 2008); (*3*) high oligomycin concentrations applied for measurement of *L* before titrations of uncoupler, when oligomycin exerts an inhibitory effect on *E*; or (*4*) loss of oxidative capacity during the time course of the respirometric assay with *E* measured subsequently to *P* (Gnaiger 2014). On the other hand, the excess ETS capacity is overestimated if non-saturating [ADP] or [Pi] (State 3) are used.

E>P is observed in many types of mitochondria and depends on: (*1*) the excess ETS capacity pushing the phosphorylation system (**Fig. 1B**) to the limit of its *capacity of utilizing* Δp_{mt}; (*2*) the pathway control state with single or multiple electron input into the Q-junction and involvement of three or less coupling sites determining the H^+_{out}/O2 *coupling stoichiometry* (**Fig. 2A**); and (*3*) the *biochemical coupling efficiency* expressed as (*E-L)/E*, since any increase of *L* causes an increase of *P* upwards to the limit of *E*. The *excess E-P* capacity, *ExP=E-P*, therefore, provides a sensitive diagnostic indicator of specific injuries of the phosphorylation system, when *E* remains constant but *P* declines relative to controls (**Fig. 6**). Substrate cocktails supporting simultaneous convergent electron transfer to the Q-junction for reconstitution of TCA cycle function stimulate ETS capacity, and consequently increase the sensitivity of the *ExP* assay.

When subtracting *L* from *P*, the dissipative LEAK component in the OXPHOS state may be overestimated. This can be avoided by measurement of LEAK respiration in a state when the protonmotive force, Δp_{mt}, is adjusted to the slightly lower value maintained in the OXPHOS state. Any turnover-dependent components of proton leak and slip, however, are underestimated under these conditions (Garlid et al. 1993). In general, it is inappropriate to use the term *ATP production* for the difference of oxygen consumption measured in states *P* and *L*. The difference *P-L* is the upper limit of the part of OXPHOS capacity which is *free* (corrected for LEAK respiration) and is fully coupled to phosphorylation with a maximum mechanistic stoichoimetry, $\approx P = P\text{-}L$ (**Fig. 6**).

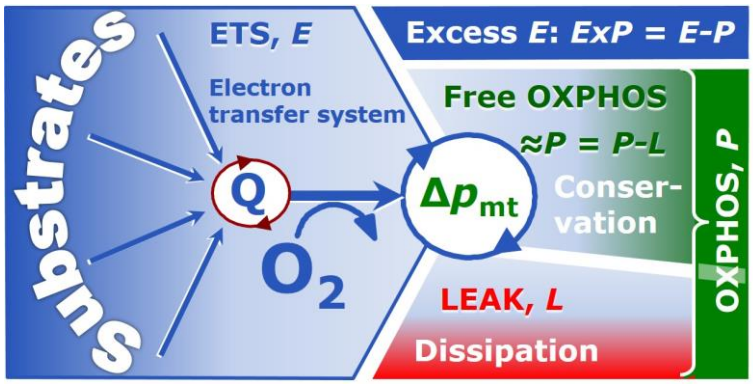

Fig. 6. Four-compartmental model of oxidative phosphorylation with respiratory states (ETS, OXPHOS, LEAK) and corresponding rates (*E*, *P*, *L*). Modified from Gnaiger (2014).

3.2. The steady-state and protonmotive force

Steady-state variables (membrane potential difference; redox states) and metabolic fluxes (*rates*) are measured in defined mitochondrial respiratory *states*. Strictly, steady states can be obtained only in open systems, in which changes due to internal transformations (*e.g.* O_2 consumption) are instantaneously compensated by external flows (*e.g.* O_2 supply), such that oxygen concentration does not change in the system (Gnaiger 1993b). Mitochondrial respiratory states monitored in closed systems may satisfy the criteria of pseudo-steady states for limited periods of time, when the changes occurring in the system (concentrations of O_2, fuel substrates, ADP) do not exert significant effects on metabolic fluxes (respiration, phosphorylation). Such pseudo-steady states require kinetically saturating concentrations of substrates to be maintained and thus depend on the kinetics of the processes under investigation.

Protonmotive force, Δp_{mt}: The protonmotive force, Δp_{mt}, across the inner mitochondrial membrane (Mitchell and Moyle 1967),

$$\Delta p_{mt} = \Delta \Psi_{mt} + \Delta \mu_{H+} / F \quad (1)$$

is composed of an electrical part, $\Delta \Psi_{mt}$, which is the difference of charge (electrical potential difference), and a chemical part, $\Delta \mu_{H+}$, which stems from the difference of pH (chemical potential difference) and incorporates the Faraday constant (**Table 3**).

Faraday constant, *F*: The Faraday constant is the product of elementary charge and the Avogadro (Loschmidt) constant, $F = e \cdot N_A$ [C/mol]. The Faraday constant yields the conversion between protonmotive force, $F_e = \Delta p_{mt}$ [J/C], expressed per *motive charge*, *e* [C], and protonmotive force or electrochemical (chemiosmotic) potential difference, $F_n = \Delta\tilde{\mu}_{H+} = \Delta p_{mt} \cdot F$ [J/mol], expressed per *motive amount of protons*, *n* [mol],

$$F_n = F_e \cdot F \tag{2}$$

In each case, the protonmotive force is expressed as the sum of two partial forces. The rather complicated symbols in Eq. 1 can be explained and visualized more easily by using *isomorphic partial protonmotive forces* (**Table 3**).

Table 3. The protonmotive force as the sum of isomorphic partial protonmotive forces (Eqs. 1 to 4). *F* is the Faraday constant (96,485.3 $C \cdot mol^{-1}$), for conversion of forces from isomorph *e* to *n*, $F_n = F_e \cdot F$.

Isomorph	Force	=	Electrical, el	+	Chemical, d	Unit
Electrical, *e*	F_e	=	$F_{e,el}$	+	$F_{e,d}$	J/C
Chemical, *n*	F_n	=	$F_{n,el}$	+	$F_{n,d}$	J/mol
Electrical, *e*	Δp_{mt}	=	$\Delta\Psi_{mt}$	+	$\Delta\mu_{H+}/F$	J/C
Chemical, *n*	$\Delta\tilde{\mu}_{H+}$	=	$\Delta\Psi_{mt} \cdot F$	+	$\Delta\mu_{H+}$	J/mol

Electrical part of the protonmotive force, el: $F_{e,el} = \Delta\Psi_{mt}$ is the electrical part of the protonmotive force expressed in units joule per coulomb, *i.e.* volt [V=J/C], defined as partial Gibbs energy change per *motive elementary charge of protons*, *e* [C].

Chemical diffusion (translocation) part of the protonmotive force, d: $F_{n,d} = \Delta\mu_{H+}$ is the chemical part of the protonmotive force expressed in units joule per mole [J/mol], defined as partial Gibbs energy change per *motive amount of protons, n* [mol].

***I*somorph *e* [C]**: $F_{e,d} = \Delta\mu_{H+}/F$ is the chemical force expressed in units joule per coulomb [J/C=V], defined as partial Gibbs energy change per *motive amount of protons expressed in units of electric charge, e* [C],

$$F_e = F_{e,el} + F_{e,d} \quad \text{[J/C]} \quad (3)$$

***I*somorph *n* [mol]:** $F_{n,el} = \Delta\Psi_{mt}\cdot F$ is the electrical force expressed in units joule per mole [J/mol], defined as partial Gibbs energy change per *motive amount of charge, n* [mol],

$$F_n = F_{n,el} + F_{n,d} \quad \text{[J/mol]} \quad (4)$$

Protonmotive means that protons are moved across the mitochondrial membrane at constant force. The direction of translocation is defined in **Fig. 2** as $H^+_{in} \rightarrow H^+_{out}$,

$$F_{n,d} = \Delta\mu_{H+} = -\ln(10)\cdot RT\cdot\Delta pH_{mt} \quad (5)$$

where RT is the gas constant times absolute temperature. $\ln(10)\cdot RT$ = 5.708 and 5.938 $kJ\cdot mol^{-1}$ at 25 and 37 °C, respectively. $\ln(10)\cdot RT/F$ = 59.16 and 61.54 mV at 25 and 37 °C, respectively. For a ΔpH of 1 unit, the chemical force (Eq. 5) changes by 6 $kJ\cdot mol^{-1}$ and the protonmotive force (Eq. 3) changes by 0.06 V.

Since F equals 96.5 $(kJ\cdot mol^{-1})/V$, a membrane potential difference of -0.2 V (Eq. 3) equals an electrochemical potential difference, $\Delta\tilde{\mu}_{H+}$, of 19 $kJ\cdot mol^{-1}$ H^+_{out} (Eq. 4). Considering a driving force of -470 $kJ\cdot mol^{-1}$ O_2 for oxidation, the thermodynamic limit of the H^+_{out}/O_2 ratio is reached at a value of 470/19 = 24, compared with a mechanistic stoichiometry of 20 (H^+_{out}/O=10).

The protonmotive force is *elevated* in the LEAK state of coupled mitochondria, driven by LEAK respiration at a minimum back flux of protons to the matrix side. Δp_{mt} is *high* in the OXPHOS state when it drives phosphorylation, and *very low* in the ETS state when uncouplers short-circuit the proton cycle.

3.3. Forces and flows in physics and irreversible thermodynamics

According to definition in physics, a potential difference and as such the *protonmotive force*, Δp_{mt}, is not a force (Cohen *et al.* 2008). The fundamental forces of physics are distinguished from *motive forces* (*e.g.* Δp_{mt}) of statistical and irreversible thermodynamics. Complementary to the attempt towards unification of fundamental forces defined in physics, the concepts of Nobel laureates Lars Onsager, Erwin Schrödinger, Ilya Prigogine and Peter Mitchell (even if expressed in apparently unrelated terms) unite the diversity of *generalized* or 'isomorphic' *flow-force* relationships, the product of which links to the dissipation function and Second Law of thermodynamics (Schrödinger 1944; Prigogine 1967). A *motive force* is the change of potentially available or 'free' energy (exergy) per isomorphic *motive* unit (force=exergy/motive unit; in integral form, this definition takes care of isothermal and non-isothermal processes). A potential difference is, in the framework of flow-force relationships, an isomorphic force, F_{tr}, involved in an exergy transformation, defined as the *partial* derivative of Gibbs energy, $\partial_{tr}G$, per advancement, $\partial_{tr}\xi$, of the transformation, tr (the isomorphic motive unit in the transformation): $F_{tr} = \partial_{tr}G/\partial_{tr}\xi$ (Gnaiger 1993a,b). This formal generalization represents an appreciation of the conceptual beauty of Peter Mitchel's innovation of the protonmotive force against the background of the established paradigm of the electromotive force (emf) defined at the limit of zero current (Cohen *et al.* 2008).

Molar quantities: 'The adjective *molar* before the name of an extensive quantity generally means *divided by amount of substance*' (Cohen *et al.* 2008). The notion that all molar quantities then become *intensive* causes ambiguity in the meaning of *molar Gibbs energy*. It is important to emphasize the fundamental difference between normalization for *amount of substance* B in a system, where $dn_B/dt \cdot V^{-1}$ is the *rate of concentration change* [$mol \cdot s^{-1} \cdot m^{-3}$], *vs.* normalization for *amount of motive substance*, where $d_r\xi_B/dt \cdot V^{-1}$ is the volume-specific flux of chemical reaction r. When the Gibbs energy of a system, G [J], is divided by the amount of substance B, n_B [mol], a *size-specific* molar quantity is obtained, G_m

= G/n_B [J·mol^{-1}], which is not an (isomorphic) force. In contrast, when the partial Gibbs energy change, $\partial_r G$ [J], is divided by the motive amount of substance B in reaction r (advancement of reaction), $\partial_r \xi_B$ [mol], the resulting *intensive* molar quantity, $F_r = \partial_r G/\partial_r \xi_B$ [J·mol^{-1}], is the chemical force of reaction r involving 1 mol B (-1 or 1, depending on B being a product or substrate, respectively).

Vectorial and scalar forces and fluxes: In chemical reactions and osmotic or diffusion processes occurring in a closed heterogeneous system, such as a chamber containing isolated mitochondria, scalar transformations occur without measured spatial direction but between separate compartments (translocation between the matrix and intermembrane space) or between energetically separated chemical substances (reactions from substrates to products). Hence the corresponding fluxes are not vectorial but scalar, and are expressed per volume and not per membrane area. The corresponding motive forces are also scalar, expressed in units [J·mol^{-1}] as potential *differences* across the membrane, without taking into account the *gradients* across the 6 nm thick inner mitochondrial membrane (Rich 1993). In a scalar electric transformation (flux of charge or current from the matrix space to the intermembrane and extramitochondrial space) the motive force is the difference of charge, $\Delta\Psi_{mt}$ [V=J·C^{-1}]. For comparison, in a mechanical, vectorial advancement, $d_{me}\xi$ [m], the unit of the *force* is newton, $\boldsymbol{F}_{me}$ [N=J·m^{-1}], and *flow* is the velocity, $\boldsymbol{v} = d_{me}\xi/dt$ [m·s^{-1}], such that the flow·force product yields mechanical power, P_{me} [W] (Cohen *et al.* 2008). The corresponding *vectorial flux* (flow density per area) is velocity per cross-sectional area [s^{-1}·m^{-1}]. The *scalar flux* lacks spatial information in a given volume, such that flux (m·s^{-1} per volume [s^{-1}·m^{-2}]) times force yields volume-specific power, P_{Vme} [W·m^{-3}].

Coupled versus bound processes: Since the chemiosmotic theory explains the mechanism of coupling in OXPHOS, it may be interesting to ask if the electrical and chemical parts of proton translocation are coupled processes. This is not the case according to the definition of coupling: Coupling occurs in an energy transformation between processes, if a

coupling mechanism allows work to be performed on the endergonic or uphill *output* process (work per unit time is power; dW/dt [J/s] = P_{out} [W]; with a positive partial Gibbs energy change) driven by the exergonic or downhill *input* process (with a negative partial Gibbs energy change). If the coupling mechanism is disengaged, the output process becomes independent of the input process, and both proceed in their downhill (exergonic) direction (**Fig. 2**). It is not possible to physically uncouple the electrical and chemical processes, which are only *theoretically* partitioned as electrical and chemical components (Eq. 3) and can be measured separately. If partial processes (fluxes, forces) are non-separable, *i.e.* cannot be uncoupled, then these are not *coupled* but are defined as *bound* processes. The electrical and chemical part of Eq. 3 are tightly bound partial forces of the protonmotive force.

Coupling, efficiency and power: In energetics (ergodynamics) coupling is defined as an exergy transformation fuelled by an exergonic (downhill) input process driving the advancement of an endergonic (uphill) output process. The (negative) output/input power ratio is the efficiency of a coupled energy transformation. Power, $P_{tr} = \partial_{tr}G/\mathrm{d}t$ [W=J·s^{-1}], is closely linked to the dissipation function (Prigogine 1967) and is the product of flow, $I_{tr}=\mathrm{d}_{tr}\xi\cdot\mathrm{d}t^{-1}$ [x_{tr}·s^{-1}] times isomorphic force, $F_{tr} = \partial_{tr}G/\partial_{tr}\xi$ [J·x_{tr}^{-1}] (Gnaiger 1993b). At the limit of maximum efficiency of a completely coupled system, the (negative) input power equals the (positive) output power, such that the total power equals zero at an efficiency of 1.

3.4. Normalization: flows and fluxes

Application of common and generally defined units is required for direct transfer of reported results into a database. The second [s] is the *SI* unit for the base quantity *time*. It is also the standard time-unit used in solution chemical kinetics. **Table 4** lists some conversion factors to obtain *SI* units. The term *rate* is too general and not useful for a database (**Fig. 7**).

Extensive quantities: An extensive quantity increases proportionally with system size. The magnitude of an extensive quantity is completely additive for non-interacting subsystems,

such as mass or flow expressed per defined system. The magnitude of these quantities depends on the extent or size of the system (Cohen *et al.* 2008).

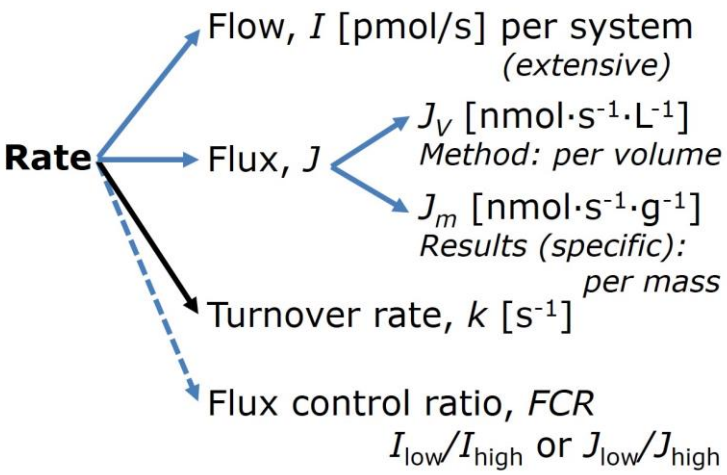

Fig. 7. Different meanings of *rate* may lead to confusion, if the normalization is not sufficiently specified. Results are frequently expressed as mass-specific *flux*, J_m, per mg protein, dry or wet weight (mass). Cell volume, V_{ce}, or mitochondrial volume, V_{mt}, may be used for normalization (volume-specific flux, J_{Vce} or J_{Vmt}), which then must be clearly distinguished from flux, J_V, expressed for methodological reasons per volume of the measurement system.

Size-specific quantities: 'The adjective *specific* before the name of an extensive quantity is often used to mean *divided by mass*' (Cohen *et al.* 2008). A mass-specific quantity (*e.g.* mass-specific flux is flow divided by mass of the system) is independent of the extent of non-interacting homogenous subsystems. Tissue-specific quantities are of fundamental interest in comparative mitochondrial physiology, where *specific* refers to the *type* rather than *mass* of the tissue. The term *specific*, therefore, must be clarified further, such that tissue mass-specific (*e.g.* muscle mass-specific) quantities are defined.

Flow per system, *I*: In analogy to electric terms, flow as an extensive quantity (*I*; per system) is distinguished from flux as a size-specific quantity (*J*; per system size) (**Fig. 7**). Electric current is a flow, I_{el} [A = C·s^{-1}], per system (extensive quantity). When dividing this extensive quantity by system size (the cross-sectional area of a wire or area of a membrane), a

size-specific quantity is obtained, which is electric flux (electric current density), $\boldsymbol{J}_{el}$ [$A \cdot m^{-2} = C \cdot s^{-1} \cdot m^{-2}$].

Size-specific flux, *J*: O_2 flow per muscle increases as muscle mass is increased. Muscle mass-specific O_2 flux should be independent of the size of the tissue sample studied in the instrumental chamber, but volume-specific O2 flux (per volume of the instrumental chamber, *V*) should increase in direct proportion to the amount of sample in the chamber. Accurate definition and reference to the *system* is decisive: the experimental system of the muscle, or the instrumental system of the measurement chamber. Volume-specific O_2 flux depends on mass-concentration of the sample in the chamber, but should be independent of chamber volume. If mass-specific O_2 flux is constant and independent of experimental system size (expressed as mass), then there is no interaction between the subsystems. A 1.5 mg and 3.0 mg muscle sample (wet weight) respires at identical mass-specific flux. The complexity changes when whole organisms are studied as experimental models. The well-established scaling law in respiratory physiology reveals a strong interaction of O_2 consumption and individual body mass of an organism, since *basal* metabolic rate (flow) does not increase linearly with body mass, whereas *maximum* mass-specific O_2 flux, $\dot{V}_{O2max}$, or $\dot{V}_{O2peak}$, is constant across a large range of individual body mass (Weibel and Hoppeler 2005). $\dot{V}_{O2peak}$ of human endurance athletes is 60 up to 80 mL $O_2 \cdot min^{-1} \cdot kg^{-1}$ body mass, converted to $J_{m,O2peak}$ of 45 to 60 $nmol \cdot s^{-1} \cdot g^{-1}$ (**Table 4**).

Flux per volume of the instrumental system, J_V: In open systems, external flows (such as O_2 supply) are distinguished from internal transformations (metabolic flow, O_2 consumption). In closed systems, external flows of all substances are zero and O_2 consumption (internal flow), I_{O2} [$pmol \cdot s^{-1}$], causes a decline of the amount of O_2 in the system, n_{O2} [nmol]. Normalization of these quantities for the volume of the system, *V* [L=dm^3], yields volume-specific O_2 flux, $J_{V,O2} = I_{O2}/V$ [$nmol \cdot s^{-1} \cdot L^{-1}$], and O_2 concentration, [O_2] or $c_{O2} = n_{O2}/V$ [$nmol \cdot mL^{-1}$=$\mu mol \cdot L^{-1}$=µM]. Volume-specific metabolic O_2 flux, $J_{V,O2}$,

depends on the specific activity and the concentration of the mitochondrial preparation in the measurement system, mtprep/*V*.

Instrumental volume-specific flux, $J_{V,O2}$, should be compared with instrumental resolution and is thus relevant mainly for methodological reasons. Normalization for sample concentration, mtprep/*V*, is required for reporting respiratory results, *e.g.* in terms of respiration per mass, W_{mtprep} (of tissue homogenate or permeabilized fibres, or mitochondrial protein), $J_{O2} = J_{V,O2}/(W_{mtprep}/V) = I_{O2}/W_{mtprep}$.

Flow per experimental model, *I*: A special case of normalization is encountered in respiratory studies with permeabilized (or intact) cells. If respiration is expressed per cell, the O_2 flow per measurement system is replaced by the O_2 flow, I_{O2}, per cell, and has frequently been expressed per 10^6 cells. Similarly, O_2 flow can be calculated from volume-specific O_2 flux, $J_{V,O2}$ [nmol·s^{-1}·L^{-1}] (per V of the measurement chamber [L]), divided by the number density of cells, $C_{ce}=N_{ce}/V$ [L^{-1}], where N_{ce} is the number of cells in the chamber. Cellular O_2 flow can be compared only between cells of identical cell size. Therefore, further normalization is important to obtain cell size-specific O_2 flux or mitochondrial marker-specific O_2 flux (Renner et al. 2003).

Many different units have been used to report the rate of oxygen consumption, OCR (**Tables 4 and 5**). For cellular studies we recommend that O_2 flow be expressed in units of attomoles (10^{-18} mol) of O_2 consumed by each cell in a second [amol·s^{-1}·cell^{-1}], equivalent to [pmol·s^{-1}·10^{-6} cells]. This convention allows information to be easily used when designing experiments in which oxygen uptake must be considered. For example, to estimate the volume-specific O_2 flux in a measurement chamber that would be expected at a particular cell density, one simply needs to multiply the flow per cell by the number of cells per volume of interest. This provides the number of moles of oxygen consumed per second in that volume. At an O_2 flow of 100 amol·s^{-1}·cell^{-1} and a cell density of 10^9 cells·L^{-1} (10^6 cells·mL^{-1}), the volume-specific O_2 flux is 100 nmol·s^{-1}·L^{-1}. Because the liter is the basic unit of volume for

concentration and is used for most solution chemical kinetics, if one multiplies $I_{ce,O2}$ by C_{ce}, then the result will not only be the moles of O_2 consumed per second in one liter, but also the change in the concentration of oxygen per second (for any volume), assuming a closed system. This is ideal for kinetic modeling as it blends with chemical rate equations where concentrations are typically expressed in $mol \cdot L^{-1}$.

Table 4. Conversion of various units used in respirometry and ergometry.

1 Unit	x	Multiplication factor	*SI*-Unit
$nmol \cdot s^{-1}$		0.09649	mA
$mA = mC \cdot s^{-1}$		10.36	$nmol \cdot s^{-1}$
ng.atom $O \cdot s^{-1}$		0.5	nmol $O_2 \cdot s^{-1}$
ng.atom $O \cdot min^{-1}$		8.33	pmol $O_2 \cdot s^{-1}$
natom $O \cdot min^{-1}$		8.33	pmol $O_2 \cdot s^{-1}$
nmol $O_2 \cdot min^{-1}$		16.67	pmol $O_2 \cdot s^{-1}$
nmol $O_2 \cdot h^{-1}$		0.2778	pmol $O_2 \cdot s^{-1}$
ml $O_2 \cdot min^{-1}$ at STPD		0.744	µmol $O_2 \cdot s^{-1}$
W = J/s at -470 kJ/mol O_2		-2.128	µmol $O_2 \cdot s^{-1}$

Table 5. Conversion for units. For prefixes see Table 6.

Name	Frequently used unit	Equivalent unit
Volume-specific flux, $J_{V,O2}$	$pmol \cdot s^{-1} \cdot mL^{-1}$	$nmol \cdot s^{-1} \cdot L^{-1}$
	$mol \cdot s^{-1} \cdot m^{-3}$	$mmol \cdot s^{-1} \cdot L^{-1}$
Cell-specific flow, I_{O2}	$pmol \cdot s^{-1} \cdot 10^{-6}$ cells	$amol \cdot s^{-1} \cdot cell^{-1}$
Cell density, C_{ce}	10^6 cells$\cdot mL^{-1}$	10^9 cells$\cdot L^{-1}$
Mass-specific flux, $J_{m,O2}$	$pmol \cdot s^{-1} \cdot mg^{-1}$	$nmol \cdot s^{-1} \cdot g^{-1}$
Catabolic power, $P_{k,O2}$	$\mu W \cdot 10^{-6}$ cells	$pW \cdot cell^{-1}$
Volume	L	dm^3
	mL	cm^3
Amount of substance concentration	$M = mol \cdot L^{-1}$	$mol \cdot dm^{-3}$

Table 6. SI prefixes (IUPAC).

Submultiple	Prefix	Symbol	Multiple	Prefix	Symbol
10^{-3}	Milli	m	10^{3}	kilo	k
10^{-6}	Micro	µ	10^{6}	mega	M
10^{-9}	Nano	n	10^{9}	giga	G
10^{-12}	Pico	p	10^{12}	tera	T
10^{-15}	Femto	f	10^{15}	peta	P
10^{-18}	Atto	a	10^{18}	exa	E
10^{-21}	zepto	z	10^{21}	zetta	Z

3.5. Conversion: oxygen, protons, ATP

J_{O2} is coupled in mitochondrial steady states to proton cycling, $J_{\infty H+} = J_{H+out} = J_{H+in}$ (**Fig. 2**). J_{H+out} and J_{H+in} [nmol·s^{-1}·L^{-1}] are converted into an electric flux (per volume), J_{el} [mC·s^{-1}·L^{-1}=mA·L^{-1}] = J_{H+out} [nmol·s^{-1}·L^{-1}]·F [C·mol^{-1}]·10^{-6} (**Table 3**). At a J_{H+out}/J_{O2} ratio or H^+_{out}/O_2 of 20 (H^+_{out}/O=10), a volume-specific O_2 flux of 100 nmol·s^{-1}·L^{-1} would correspond to a proton flux of 2,000 nmol H^+_{out}·s^{-1}·L^{-1} or volume-specific current of 193 mA·L^{-1}.

$$J_e \text{ [mA·L}^{-1}\text{]} = J_{H+out}\cdot F\cdot 10^{-6} \text{ [nmol·s}^{-1}\text{·L}^{-1}\text{·mC·nmol}^{-1}\text{]} \quad (6.1)$$

$$J_e \text{ [mA·L}^{-1}\text{]} = J_{V,O2}\cdot(H^+_{out}/O_2)\cdot F\cdot 10^{-6} \text{ [mC·s}^{-1}\text{·L}^{-1}\text{=mA·L}^{-1}\text{]} \quad (6.2)$$

ETS capacity in various human cell types including HEK 293, primary HUVEC and fibroblasts ranges from 50 to 180 amol·s^{-1}·cell^{-1} (see Gnaiger 2014). At 100 amol·s^{-1}·cell^{-1} corrected for ROX (corresponding to a catabolic power of -48 pW·cell^{-1}), the current across the mt-membranes, I_e, approximates 193 pA·cell^{-1} or 0.2 nA per cell. See Rich (2003) for an extension of quantitative bioenergetics from the molecular to the human scale, with a transmembrane proton flux equivalent to 520 A in an adult at a catabolic power of -110 W.

For NADH- and succinate-linked respiration, the mechanistic »P/O_2 ratio (referring to the full 4 electron reduction of O_2) is calculated at 20/3.7 and 12/3.7 (Eq. 7) equal to 5.4 and 3.3. The classical »P/O ratios (referring to the 2 electron reduction of 0.5 O_2) are 2.7 and 1.6 (Watt et al. 2010), in direct agreement with the measured »P/O ratio for succinate of 1.58 ±

0.02 (Gnaiger et al. 2000; for detailed reviews see Wikström and Hummer 2012; Sazanov 2015),

$$»P/O_2 = (H^+_{out}/O_2)/(H^+_{in}/»P) \quad (7)$$

In summary (**Fig. 1**),

$$J_{V,»P}\ [nmol \cdot s^{-1} \cdot L^{-1}] = J_{V,O2} \cdot (H^+_{out}/O_2)/(\ H^+_{in}/»P) \quad (8.1)$$

$$J_{V,»P}\ [nmol \cdot s^{-1} \cdot L^{-1}] = J_{V,O2} \cdot (»P/O_2) \quad (8.2)$$

Considering isolated mitochondria as powerhouses and proton pumps as molecular machines and relating the experimental results to energy metabolism of the intact cell, the cellular $»P/O_2$ based on oxidation of glycogen is increased by the glycolytic substrate-level phosphorylation of 3 »P/Glyc. Addition the equivalent of 0.5 to the mitochondrial $»P/O_2$ ratio of 5.4 yields a bioenergetic cell physiological $»P/O_2$ ratio close to 6. Two NADH equivalents are formed during glycolysis and transported from the cytosol into the mitochondrial matrix, the energetic cost of which must potentially be taken into account. Taking also into account the substrate-level phosphorylation in the TCA cycle, this high $»P/O_2$ ratio not only reflects proton translocation and OXPHOS studied in isolation, but integrates mitochondrial physiology with energy transformation in the living cell (Gnaiger 1993b).

4. Conclusions

MitoEAGLE can serve as a gateway to better diagnose mitochondrial respiratory defects, which are linked to genetic variations, age-related health risks, gender-specific mitochondrial performance, life style with its consequences on degenerative diseases, and environmental exposure to toxicological agents. The present recommendations on coupling control (Part 1) will be extended in a series of manuscripts to pathway control of mitochondrial respiration, substrate-uncoupler-inhibitor-titration (SUIT) protocols and the harmonization of experimental procedures.

The optimal choice for expressing O_2 flow per biological system, and normalization for specific tissue-markers (volume, mass, protein) and mitochondrial markers (volume, protein, content, mtDNA, activity of marker enzymes) is guided by the scientific question. Interpretation of the data obtained depends critically on the appropriate normalization, and reporting rates merely as nmol·s^{-1} is discouraged. For studies with intact or permeabilized cells, we recommend that normalizations be provided as far as possible: (*1*) on a per cell basis as O_2 flow (a biophysical normalization); (*2*) per mg cell protein or per cell mass as mass-specific O_2 flux (a cellular normalization); and (*3*) per mitochondrial marker as mt-specific flux (a mitochondrial normalization). With information on cell size and the use of both normalizations the maximal potential information is available (Renner *et al.* 2003; Wagner *et al.* 2011; Gnaiger 2014).

To provide an overall perspective of mitochondrial physiology we may link cellular bioenergetics to systemic human respiratory activity, without yet addressing cell- and tissue-specific mitochondrial function. A routine O_2 flow of 234 μmol·s^{-1} per individual or flux of 3.3 nmol·s^{-1}·g^{-1} body mass corresponds to -110 W catabolic energy flow at a body mass of 70 kg and -470 kJ/mol O_2. Considering a cell count of $514 \cdot 10^6$ cells per g tissue mass and an estimate of 300 mitochondria per cell (Ahluwalia 2017), the average O_2 flow per cell at $J_{m,O2peak}$ of 45 nmol·s^{-1}·g^{-1} (60 ml O_2·min^{-1}·kg^{-1}) is 88 amol·s^{-1}·cell^{-1}, which compares well with OXPHOS capacity of human fibroblasts (not ETS but the lower OXPHOS capacity is used as a reference; Gnaiger 2014). We can describe our body as the sum of $36 \cdot 10^{12}$ cells (36 trillion cells). Mitochondrial fitness of our $11 \cdot 10^{15}$ mitochondria (11 quadrillion mt) is indicated if O_2 flow of 0.02 amol·s^{-1}·mt^{-1} at rest can be activated to 0.3 amol·s^{-1}·mt^{-1} at high ergometric performance.

References (*incomplete; www links will be deleted in the final version*)

Ahluwalia A. Allometric scaling in-vitro. Sci Rep 2017;7:42113.

Altmann R. Die Elementarorganismen und ihre Beziehungen zu den Zellen. Zweite vermehrte Auflage. Verlag Von Veit & Comp, Leipzig 1894;160 pp. - www.mitoeagle.org/index.php/Altmann_1894_Verlag_Von_Veit_%26_Comp

Brown GC. Control of respiration and ATP synthesis in mammalian mitochondria and cells. Biochem J 1992;284:1-13. - www.mitoeagle.org/index.php/Brown_1992_Biochem_J

Chance B, Williams GR. Respiratory enzymes in oxidative phosphorylation: III. The steady state. J Biol Chem 1955;217:409-27. - www.mitoeagle.org/index.php/Chance_1955_J_Biol_Chem-III

Chance B, Williams GR. Respiratory enzymes in oxidative phosphorylation. IV. The respiratory chain. J Biol Chem 1955;217:429-38. - www.mitoeagle.org/index.php/Chance_1955_J_Biol_Chem-IV

Chance B, Williams GR. The respiratory chain and oxidative phosphorylation. Adv Enzymol Relat Subj Biochem 1956;17:65-134. - www.mitoeagle.org/index.php/Chance_1956_Adv_Enzymol_Relat_Subj_Biochem

Cohen ER, Cvitas T, Frey JG, Holmström B, Kuchitsu K, Marquardt R, Mills I, Pavese F, Quack M, Stohner J, Strauss HL, Takami M, Thor HL. Quantities, Units and Symbols in Physical Chemistry, IUPAC Green Book 2008;3rd Edition, 2nd Printing, IUPAC & RSC Publishing, Cambridge. - www.mitoeagle.org/index.php/Cohen_2008_IUPAC_Green_Book

Ernster L, Schatz G Mitochondria: a historical review. J Cell Biol 1981;91:227s-55s. - www.mitoeagle.org/index.php/Ernster_1981_J_Cell_Biol

Estabrook RW. Mitochondrial respiratory control and the polarographic measurement of ADP:O ratios. Methods Enzymol 1967;10:41-7. - www.mitoeagle.org/index.php/Estabrook_1967_Methods_Enzymol

Fell D. Understanding the control of metabolism. Portland Press 1997.

Garlid KD, Semrad C, Zinchenko V. Does redox slip contribute significantly to mitochondrial respiration? In: Schuster S, Rigoulet M, Ouhabi R, Mazat J-P (eds) Modern trends in biothermokinetics. Plenum Press, New York, London 1993;287-93.

Gnaiger E. Efficiency and power strategies under hypoxia. Is low efficiency at high glycolytic ATP production a paradox? In: Surviving Hypoxia: Mechanisms of Control and Adaptation. Hochachka PW, Lutz PL, Sick T, Rosenthal M, Van den Thillart G (eds.) CRC Press, Boca Raton, Ann Arbor, London, Tokyo 1993a:77-109. - www.mitoeagle.org/index.php/Gnaiger_1993_Hypoxia

Gnaiger E. Nonequilibrium thermodynamics of energy transformations. Pure Appl Chem 1993b;65:1983-2002. - www.mitoeagle.org/index.php/Gnaiger_1993_Pure_Appl_Chem

Gnaiger E. Bioenergetics at low oxygen: dependence of respiration and phosphorylation on oxygen and adenosine diphosphate supply. Respir Physiol 2001;128:277-97. - www.mitoeagle.org/index.php/Gnaiger_2001_Respir_Physiol

Gnaiger E. Mitochondrial pathways and respiratory control. An introduction to OXPHOS analysis. 4th ed. Mitochondr Physiol Network 2014;19.12. Oroboros MiPNet Publications, Innsbruck:80 pp. - www.mitoeagle.org/index.php/Gnaiger_2014_MitoPathways

Gnaiger E. Capacity of oxidative phosphorylation in human skeletal muscle. New perspectives of mitochondrial physiology. Int J Biochem Cell Biol 2009;41:1837-45. - www.mitoeagle.org/index.php/Gnaiger_2009_Int_J_Biochem_Cell_Biol

Gnaiger E, Méndez G, Hand SC. High phosphorylation efficiency and depression of uncoupled respiration in mitochondria under hypoxia. Proc Natl Acad Sci USA 2000;97:11080-5. - www.mitoeagle.org/index.php/Gnaiger_2000_Proc_Natl_Acad_Sci_U_S_A

Hofstadter DR. Gödel, Escher, Bach: An eternal golden braid. A metaphorical fugue on minds and machines in the spirit of Lewis Carroll. Harvester Press 1979;499 pp. - www.mitoeagle.org/index.php/Hofstadter_1979_Harvester_Press

Komlódi T, Tretter L. Methylene blue stimulates substrate-level phosphorylation catalysed by succinyl-CoA ligase in the citric acid cycle. Neuropharmacology 2017;123:287-98. - www.mitoeagle.org/index.php/Komlodi_2017_Neuropharmacology

Lemieux H, Blier PU, Gnaiger E. Remodeling pathway control of mitochondrial respiratory capacity by temperature in mouse heart: electron flow through the Q-junction in permeabilized fibers. Sci Rep 2017;7:2840. - www.mitoeagle.org/index.php/Lemieux_2017_Sci_Rep

Miller GA. The science of words. Scientific American Library New York 1991;276 pp. - www.mitoeagle.org/index.php/Miller_1991_Scientific_American_Library

Mitchell P, Moyle J. Respiration-driven proton translocation in rat liver mitochondria. Biochem J 1967;105:1147-62. - www.mitoeagle.org/index.php/Mitchell_1967_Biochem_J

Morrow RM, Picard M, Derbeneva O, Leipzig J, McManus MJ, Gouspillou G, Barbat-Artigas S, Dos Santos C, Hepple RT, Murdock DG, Wallace DC. Mitochondrial energy deficiency leads to hyperproliferation of skeletal muscle mitochondria and enhanced insulin sensitivity. Proc Natl Acad Sci U S A 2017;114:2705-10. - www.mitoeagle.org/index.php/Morrow_2017_Proc_Natl_Acad_Sci_U_S_A

Prigogine I. Introduction to thermodynamics of irreversible processes. Interscience, New York, 1967;3rd ed.

Puchowicz MA, Varnes ME, Cohen BH, Friedman NR, Kerr DS, Hoppel CL. Oxidative phosphorylation analysis: assessing the integrated functional activity of human skeletal muscle mitochondria – case studies. Mitochondrion 2004;4:377-85. - www.mitoeagle.org/index.php/Puchowicz_2004_Mitochondrion

Renner K, Amberger A, Konwalinka G, Gnaiger E. Changes of mitochondrial respiration, mitochondrial content and cell size after induction of apoptosis in leukemia cells. Biochim Biophys Acta 2003;1642:115-23. - www.mitoeagle.org/index.php/Renner_2003_Biochim_Biophys_Acta

Rich P. Chemiosmotic coupling: The cost of living. Nature 2003;421:583. - www.mitoeagle.org/index.php/Rich_2003_Nature

Rostovtseva TK, Sheldon KL, Hassanzadeh E, Monge C, Saks V, Bezrukov SM, Sackett DL. Tubulin binding blocks mitochondrial voltage-dependent anion channel and regulates respiration. Proc Natl Acad Sci USA 2008;105:18746-51. - www.mitoeagle.org/index.php/Rostovtseva_2008_Proc_Natl_Acad_Sci_U_S_A

Rustin P, Parfait B, Chretien D, Bourgeron T, Djouadi F, Bastin J, Rötig A, Munnich A. Fluxes of nicotinamide adenine dinucleotides through mitochondrial membranes in human cultured cells. J Biol Chem 1996;271:14785-90.

Sazanov LA. A giant molecular proton pump: structure and mechanism of respiratory complex I. Nat Rev Mol Cell Biol 2015;16:375-88. - www.mitoeagle.org/index.php/Sazanov_2015_Nat_Rev_Mol_Cell_Biol

Schrödinger E. What is life? The physical aspect of the living cell. Cambridge Univ Press, 1944. - www.mitoeagle.org/index.php/Gnaiger_1994_BTK

Wagner BA, Venkataraman S, Buettner GR. The rate of oxygen utilization by cells. Free Radic Biol Med. 2011:51:700-712. http://dx.doi.org/10.1016/j.freeradbiomed.2011.05.024 PMCID: PMC3147247

Watt IN, Montgomery MG, Runswick MJ, Leslie AG, Walker JE. Bioenergetic cost of making an adenosine triphosphate molecule in animal mitochondria. Proc Natl Acad Sci U S A 2010;107:16823-7. - www.mitoeagle.org/index.php/Watt_2010_Proc_Natl_Acad_Sci_U_S_A

Weibel ER, Hoppeler H. Exercise-induced maximal metabolic rate scales with muscle aerobic capacity. J Exp Biol 2005;208:1635–44.

Wikström M, Hummer G. Stoichiometry of proton translocation by respiratory complex I and its mechanistic implications. Proc Natl Acad Sci U S A 2012;109:4431-6. - www.mitoeagle.org/index.php/Wikstroem_2012_Proc_Natl_Acad_Sci_U_S_A